Vol 12 No 10, October 2003
1009-1963/2003/12(10)/1076-011

Chinese Physics

© 2003 Chin. Phys. Soc.
and IOP Publishing Ltd

Evaluation of the applicability of a retrospective scheme based on comparison with several difference schemes*

Feng Guo-Lin(封国林)[a)b)] and Dong Wen-Jie(董文杰)[c)]

[a)] *Mathematics and Physics College, Yangzhou University, Yangzhou* 225009, *China*

[b)] *Institute of Atmospheric Physics, Chinese Academy of Sciences, Beijing* 100029, *China*

[c)] *National Climate Centre of China, Beijing* 100080, *China*

(Received 29 September 2002; revised manuscript received 8 May 2003)

The evaluation of the applicability of a retrospective multi-time-level scheme (RT scheme) is carried out on the basis of comparison with the common leapfrog scheme (LF scheme) and its derivatives, and modified BOTT's positive-definite schemes used in atmospheric models. Two rational flow field tests confirm that at least the BOTT scheme tested may be applied, but apparently the best results are obtained by the RT scheme. The results of wavelet analysis show that the RT scheme can better extract the useful information from the initial fields, i.e. to memorize many main initial characteristics, such as periods, thus offering a new approach to the short-term climate numerical prediction.

Keywords: short-term climate prediction, difference scheme, advection equation, retrospective multi-time-level scheme

PACC: 0530, 0540

1. Introduction

An important domain of numerical analysis is the solution of the linear pure advection equation, which describes the transport of particular quantities in a given field, and plays a major role in the numerical modelling of atmospheric processes and other geophysical phenomena. Because this problem is linear, the hyperbolic property and initial condition discontinuities and other non-smooth features are retained,[1] which imposes serious numerical computational problems such as the creation of numerical diffusion and/or dispersive waves (dispersion). Most existing numerical approximations tend to smear and smooth such discontinuous features, therefore an important task faced is to reduce or eliminate the numerical dispersion problem while keeping computational economy in numerical calculation and analysis. In applications such as in atmospheric or water pollution models, the advection plays a major role in mass transport. The search for an efficient scheme has been an important and active topic in the domain of numerical computation. Numerous articles on this subject have been published; for example, James,[2] and Feng *et al*[3,4] Liu *et al*[5] put forward a lattice Boltzmann method for two-dimensional (2D) convection. Cao *et al*[6] discussed the conditions of stability and convergence of the six-point weighted difference scheme for the generalized nonlinear Schrödinger equation. In terms of statistical physics, a fluid such as air is a many-body system; it has a vast amount of degrees of freedom and thus obeys the second law of thermodynamics. Liu *et al*[7,8] made a notable improvement in prognostic outputs by reconstructing the terms of horizontal diffusion in a nested grid version of PSU/NCAR's mesoscale model (MM5) according to the principles of the second law of thermodynamics; besides, the computational noise was effectively and significantly suppressed since the physical dissipative technique in the reconstruction was based on the physical law rather than on the computational method such as the artificial viscosity.

*Project supported by the National Natural Science Foundation of China (Grant Nos 40275031 and 40231006), the State Key Development Program for Basic Research (Grant No G1999043408) and the K. C. Wong Education Foundation, Hong Kong.

A wide range of numerical schemes has been developed to solve nonlinear differential equations.[9,10] In addition to the well-known schemes based on difference approximation, new methods have been developed over the past decade. These methods enable the solution of specific problems in hydrodynamics, aerodynamics, and astronomy as they provide an accurate description of discontinuous solutions. In past decades, a large variety of different methods has been developed for the numerical solution of the transport equation in atmospheric models, such as the Crowley conservative advection scheme,[11] which was popular in the domain of numerical computation because of its second-order accuracy in both space and time and its storage requirement of only one time-level,[12] and the common leapfrog scheme (LF scheme) and its derivatives, the non-positive-definite numerical scheme was completed by the flux transport limiter as formulated by BOTT, hereafter BOTT schemes[13−16] and so on. However, many of these advection schemes show different disadvantages, and sometimes produce large computational errors. For instance, the upstream method on the one hand is known to be very diffusive[13] and on the other hand, multi-time values before the initial time are required in solving the ordinary differential equation with linear multi-step method; and these values are still computed from the given initial value by using one of above-mentioned schemes. That is to say, the one initial value principle is invariably abided in numerical computation. Namely, the numerical integration uses only one time-level initial value of past observational data. The retrospective multi-time-level integral scheme (RT scheme), which we have proposed and discussed in detail,[17−20] has overcome the above-mentioned defects.

Based on the atmospheric self-memorization principle, the RT scheme has been adopted in MM5, the concrete expression of model is derived, and called the self-memory MM5 model (hereafter SMM5), for the purpose to apply the scheme to MM5 and to validate the efficiency of the scheme, and the experimental results have been compared with those of kernel model MM5. The comparison showed that because of extracting the information of several time-level history fields, SMM5 improved the prediction accuracy. As to the rainfall field, both the areas and intensities of precipitation in SMM5 were more similar to the observed field than those in MM5.[21]

This paper presents the accuracy and computational efficiency of the RT scheme in comparison with the several common difference schemes used in meteorological models to investigate and evaluate its performance. The relations between the computational time consumption and their accuracy determine the efficiency of the schemes which is expressed in commonly defined norms and other skills such as correlation coefficients, rates of same sign. Two commonly used simple rotational flow-field tests are applied to compare the schemes in this paper. The LF2, LF2C and BOTT schemes are referred to Ref.[22], and the RT scheme to Ref.[17], respectively.

(1) LF2 — the common leapfrog scheme of the second order (centred in time and in space) completed by an Asselin filter $\beta^t = (1-2\gamma)\alpha^t + \gamma(\alpha^{t+1} + \beta^{t-1})$, where the upper index denotes the time-level and the variable β denotes the smoothed values. The filter parameter γ was set to 0.10 in the calculations.

(2) LF2C — the same method as in (1) completed by the flux transport limiter derived by Smolarkiewicz.[23]

(3) BOTT — a modification of the original BOTT's positive-definite scheme with polynomial approximation to the fourth order.[13] The original version appeared slightly unstable in the deformational flow-field test integrated for a long time interval. The scheme was later modified by Bott[14−16] and Easter.[24] In our tests, we used another simple modification of the original scheme, which uses Easter's equations[24] for calculation of $c_{i+1/2}$[13],

$$c_{i+1/2} = \frac{\Delta t}{\Delta x} u_{i+1/2} \Big/ \left(1 + 0.5 \frac{\Delta t}{\Delta x}(u_{i+1/2} - u_{i-1/2})\right),$$

where Δt, Δx, u and i represent time increment, grid step, advection velocity and grid-point index, respectively. This modification is very simple and improves the results of the deformational flow-field test integration for a long time interval.

(4) RT — a new multi-time-level scheme including the past observational data, which has both the integration and filtering functions. This is a very simple method and improves the results of the numerical regional climate model integrated for a long-term, due to its better memory of initial field information.

2. Numerical tests

We need to define an error between the predicted and actual trajectories of a system so as to measure the accuracy of the prediction model within the range of locality assumption. The correlation coefficients (C_R) between predicted and actual/ ideal fields, and the rate of same sign (R) are adopted in this paper,

$$C_R = \frac{\frac{1}{N}\sum_{i=1}^{N}(x_i-\overline{x})(y_i-\overline{y})}{\sqrt{\frac{1}{N}\sum_{i=1}^{N}(x_i-\overline{x})^2}\sqrt{\frac{1}{N}\sum_{i=1}^{N}(y_i-\overline{y})^2}}, \quad (1)$$

$$R = \frac{\sum n_i}{N} \times 100\%. \quad (2)$$

If the sign of predicted value coincides with that of the ideal value, n_i=1, otherwise n_i=0. N is the total number of grid points in the space.

The tests were performed in a square domain with an equidistant grid step in both directions. Their norms were used as a measure of accuracy,

$$\|e\|_\infty = \max_{i,j=1,N}|e_{ij}|,$$
$$\|e\|_1 = \frac{1}{N^2}\sum_{i,j=1}^{N}|e_{i,j}|,$$
$$\|e\|_2 = \frac{1}{N}\left(\sum_{i,j=1}^{N} e_{i,j}^2\right)^{0.5}. \quad (3)$$

Similar to Ref.[21], the numerical tests were used to compare the accuracy and computational efficiency of the schemes. In this paper, the efficiency is determined by evaluating the computational time required by a scheme to reach a prescribed accuracy, which depends on the computational platform used, construction and optimization of the code, and on the test formulations. Our tests were performed on a personal computer (PC) with a single central processing unit (CPU) (Pentium Pro 933 MHz), the program codes were programmed without special optimization and single precisions was used in numerical computation.

2.1. Rotational flow-field test for the initial sine waves

A rotational flow-field test of initial sine waves serves as a comparison of the accuracy and computational efficiency of the schemes. The linear advection equation is written as

$$\frac{\partial u}{\partial t} + C\frac{\partial u}{\partial x} + C\frac{\partial u}{\partial y} = 0,$$

$$-1 \le x \le 1, \quad 1 \le y \le 1, \quad (4)$$

and its analytic solution takes the form

$$u(x,y,t) = A\sin\left[\frac{2\pi}{T_\mathrm{p}}(x+y) + 2Ct\right], \quad (5)$$

where $x_i = i\Delta x$, $y_j = j\Delta y$, $\Delta x = \Delta y = 0.01$; $t_\tau = 0.01\tau$; C=1.0, and T_p is the period of the initial sine wave.

Obviously, Eq.(5) is composed of sine and cosine. If x, y are given, u varies with time t. The series of the first 50 time-steps generated by Eq.(5) were taken as a dependent sample, i.e. a real time series, and the memory coefficients of the RT scheme were obtained from the real time series which served as the initial fields. The time-step was Δt=0.1Δx=0.001 in the LF2, LF2C and BOTT schemes so as to satisfy the conditional stability under the initial condition $u(x,y,t_0) = A\sin\left[\frac{2\pi}{T_\mathrm{p}}(x+y) + 2Ct_0\right]$, t_0=0.49, however, the time-step in the RT scheme was 0.01, which was ten times that in the other schemes. In the numerical experiments, the computational domain was covered by $N\times N$ grid points, and the numerical solutions of Eq.(4) were obtained using the respective abovementioned schemes. In order to evaluate the schemes' applicability, the ideal field was obtained from Eq.(5), and the variable curves for C_R, R and three error norms from t=0 to t=1.0 were calculated according to formulae defined by Eqs.(1)–(3). The main results obtained in the first test for N=21 are given in Fig.1.

With increasing integration time the correlation coefficient C_R for the RT scheme decreases slowly from 0.82 at t=0 to 0.24 at t=1.0 (see Fig.1 (a)). The C_R curve for the BOTT scheme increases from 0.42 to the maximum 0.50 in the integration interval [0.0, 0.20], then drops slowly to –0.35 at t=1.0. The variation tendency of the curve for the LF2C scheme is opposite to that of the BOTT, it drops slowly from 0.24 at t=0.0 to the minimum –0.18 at t=0.60, then increases slowly up to 0.004 at the end of integration t=1.0. The C_R for the LF2 scheme is the same as that for the RT scheme at the beginning, but drops rapidly to the minimum –0.60 at the end of integration t=1.0. A very interesting thing is that the C_R for the BOTT, and LF2 intersect with that of LF2C scheme at $t \sim 0.70$ when their values are about –0.10, then the curve for the LF2C scheme slowly rises, while the others continue to drop. The difference between BOTT and LF2 schemes is that the down slopes of correlation coefficient curve for the former is smaller than that for the latter.

Figure 1(b) shows the variation of the rate of same sign between predicted and ideal fields for the four schemes, and all of them show obviously the characteristic oscillation phenomenon. At t=1.0, the accuracy of the RT, BOTT, LF2C and LF2 schemes is 65%, 45%, 45% and 25%, respectively. Without doubt, the RT scheme is most accurate, while the worst is the LF2 scheme. The close resemblance of the results of the LF2C and BOTT schemes is a general feature. Their curves are relatively close, and nearly overlap in the time interval [0.68, 1.00]. Figure 1(c) shows that the greatest error norm of the RT scheme constantly maintains the value of about 1.0, but increases sharply from 1.0 to 1.74 in the last 50 time steps from t=0.50 to t=1.0. The greatest error curve of the BOTT scheme shows a variable tendency of three obvious different sections in the integration interval: it maintains the values of about 1.25 in the interval [0.001,0.450], and increases from 1.25 to 1.85 rapidly in [0.450,0.650], then oscillates around 1.85 in [0.650,1.00]. The variation tendencies of the LF2C and LF2 schemes are similar to the BOTT scheme, but the greatest error of the former increases faster than the latter.

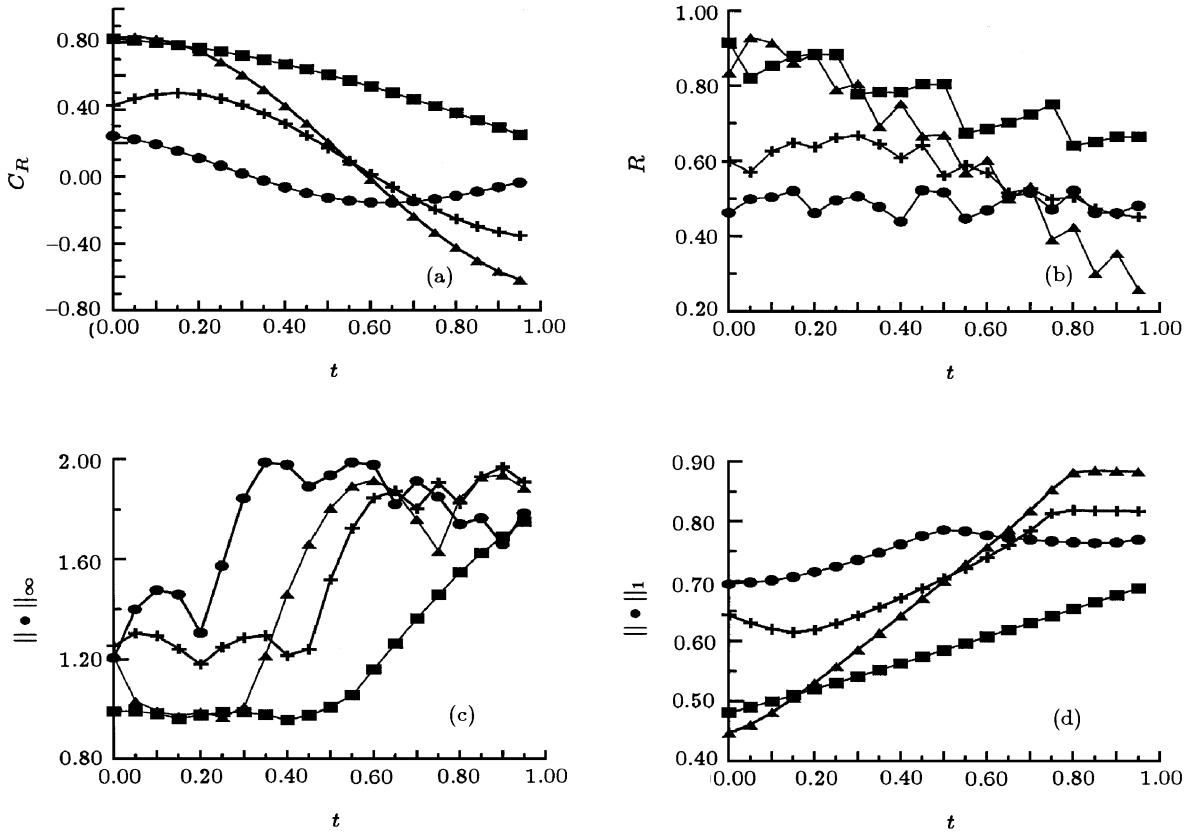


Fig.1. Temporal variations of prediction skills (correlation coefficients (a), and rates of same sign (b)), and errors expressed in $\|\bullet\|_\infty$ (c), and $\|\bullet\|_1$ (d) norms in the first test, their initial field being given by Eq.(5). The time increment is 0.01 for the RT scheme, and 0.001 for the others. —■— RT, —+— BOTT, —•— LF2C, —▲— LF2.

The temporal evolution of the minimum errors $\|\bullet\|_1$ (Fig.1(d)) is similar to that of the root-mean-square errors $\|\bullet\|_2$ (figure omitted) defined by Eq.(3). The minimum error of the LF2 scheme increases most rapidly, and finally stays at about 0.85. For a short-term integration, the $\|\bullet\|_1$ and $\|\bullet\|_2$ norms of the LF2C scheme are larger than those of the BOTT scheme, and according to the norm definitions, the BOTT scheme has an advantage over the LF2C scheme; but for a long-term integration, the $\|\bullet\|_1$ norm of the former continues rising, while that of the latter starts dropping.

The results obtained from the first test for N=21 are summarized in Table 1.

Table 1. Results of the first rational field test for N=21 with the four schemes.

Scheme	Δt	$U_{\min}$	$U_{\max}$	C_R	p_c	R	p_R	$\| \bullet \|_\infty$	p_∞	$\| \bullet \|_1$	p_1	$\| \bullet \|_2$	p_2	t_c/s
RT	0.010	0	8.18	1.00	1	1.00	1	7.18	1	0.60	1	0.67	1	5.11
LF2	0.001	0	6.43	0.04	4	0.93	3	8.19	4	0.79	4	0.89	4	0.36
LF2C	0.001	–0.02	6.08	0.44	3	0.90	4	8.17	3	0.67	3	0.76	2	0.39
BOTT	0.001	–0.47	5.83	0.84	2	0.99	2	7.86	2	0.71	2	0.83	3	1.03

Table 1 contains the time step (Δt), minimum ($U_{\min}$) and maximum ($U_{\max}$) values, errors expressed in the norms ($\| \bullet \|_\infty$, $\| \bullet \|_1$ and $\| \bullet \|_2$) and the time consumption (t_c) of the integration. The columns p_c, p_R, p_∞, p_1 and p_2 denote the relative performance of the scheme in the corresponding prediction skills and error norms.

Generally, the smallest errors were obtained by the RT scheme. For the retrospective order $p \geq 3$, the RT scheme provided the smallest error in all norms and the greatest correlation coefficients and rate of same sign, and its preference increases with p. This may be attributed to its filtering function in comparison with the other schemes. The second best results were obtained by the BOTT scheme, which uses the high polynomial approximation. The LF2 and LF2C schemes were the worst, which is due to their smaller diffusion and greater dispersion in comparison with the RT scheme.

Spool[22] suggested that the test could be applied in two ways. Short-term integration may be used to evaluate the accuracy of the schemes. Long-term integration serves as a strength test of nonlinear instability of the scheme because, after a certain integration time, the analytic solution produces bounded effect on the given grid.

However, for a long-term integration, e.g. t=500, we found that the correlation coefficient and same sign rate between the predicted field obtained by the application of the LF2, LF2C, BOTT and RT schemes and the ideal field yielded by Eq.(5) show a quasi-periodic wave phenomenon. The relations between the periods of the initial field and the oscillations of the curves obtained by the RT and LF2 schemes, respectively, are carefully studied in this paper. In the test, the period T_p of the initial field of Eq.(5) was given as 4, 6, 8,10 and 20, respectively, and the numerical solutions of Eq.(4) from t=0 to t=500 were obtained by using the RT and LF2 schemes. And then the analysis period of the time series of the correlation coefficient defined in Eq.(1) was obtained by the wavelet analysis method.

The periods of the numerical solutions obtained by the LF2 scheme have hardly any relation with the initial fields, because the effect of computational solution has made the numerical solutions lose the most of the initial information (see Fig.2).

However, Fig.3 shows that the analysis periods of the time series obtained by the application of the RT scheme have a very fine correspondence to those of the initial fields, which are due to its utilization of the past initial information. It may be the reason that the long-term forecast may be made with the RT scheme.

2.2. Rotational flow-field test

The initial flow-field of the second test is one of exponential type. The analytical solution of Eq.(4) takes the form

$$u(x, y, t) = A \exp[B(x + y) + 2Ct], \tag{6}$$

where $x_i = i\Delta x$, $y_j = j\Delta y$, $\Delta x = \Delta y = 0.01$, $t_\tau = 0.01\tau$, C=1.0, and A, B are constants. In the second experiment, the main features of the results obtained by the four schemes are similar to the first test for N=21, and summarized in Table 2.

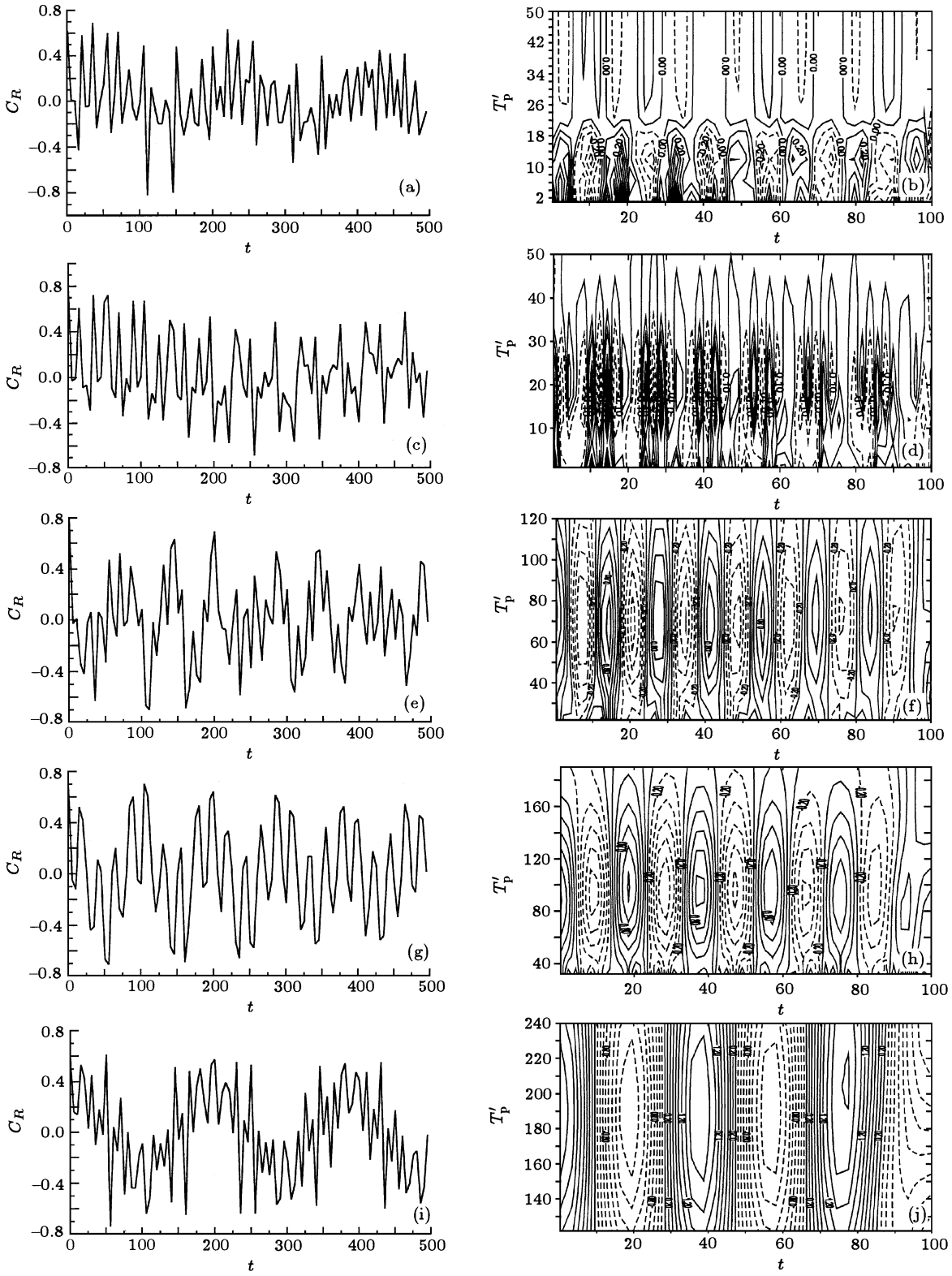


Fig.2. Temporal variations of the correlation coefficients (time series) from t=0 to t=500 (corresponding to 500000 time-steps) obtained by the application of the LF2 scheme, and the corresponding analysis periods of the time series obtained by the wavelet analysis method. T_p and T'_p denote the periods of the initial field and the time series, respectively. The abscissa units of (b), (d), (f), (h), (j) are 1×5, and the ordinate represents various analysis periods; the other abscissa (a), (c), (e), (g), (i) denotes the integration time t and the other ordinate the correlation coefficient. (a) for T_p=4, (b) for T'_p=12, (c) for T_p=6, (d) for T'_p=18, (e) for T_p=8, (f) for T'_p=70, (g) for T_p=10, (h) for T'_p=100, (i) for T_p=20, (j) for T'_p=190.

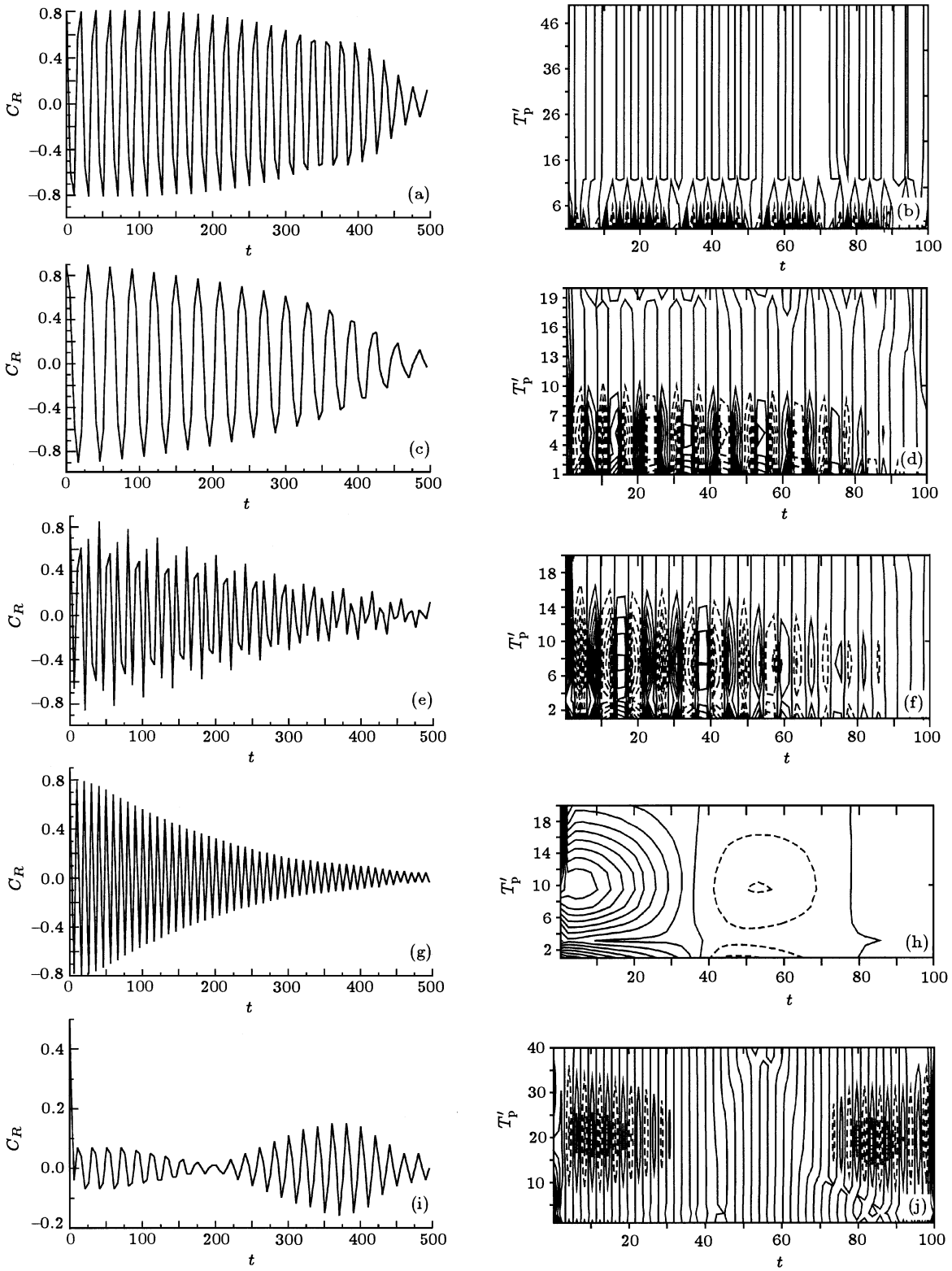


Fig.3. As in Fig.2, except obtained by the RT scheme and with the time increment being 0.01, corresponding to 50000 time steps in the total. (a) for T_p=4, (b) for T'_p=4, (c) for T_p=6, (d) for T'_p=6, (e) for T_p=8, (f) for T'_p=8, (g) for T_p=10, (h) for T'_p=10, (i) for T_p=20, (j) for T'_p=20.

Table 2. Results of the second rational flow-field test for N=21 with the four schemes.

Scheme	Δt	$U_{\min}$	$U_{\max}$	C_R	p_c	R	p_R	$\|\bullet\|_\infty$	p_∞	$\|\bullet\|_1$	p_1	$\|\bullet\|_2$	p_2	t_c/s
RT	0.010	–0.09	13.5	0.89	1	0.95	1	7.19	1	1.59	4	2.04	3	3.11
LF2	0.001	–11.9	32.1	0.45	4	0.76	3	8.23	4	1.49	2	2.08	4	0.26
LF2C	0.001	–7.67	21.9	0.41	3	0.79	4	8.25	3	1.49	1	2.03	2	0.31
BOTT	0.001	–6.08	13.3	0.81	2	0.92	2	7.93	2	1.51	3	1.99	1	1.23

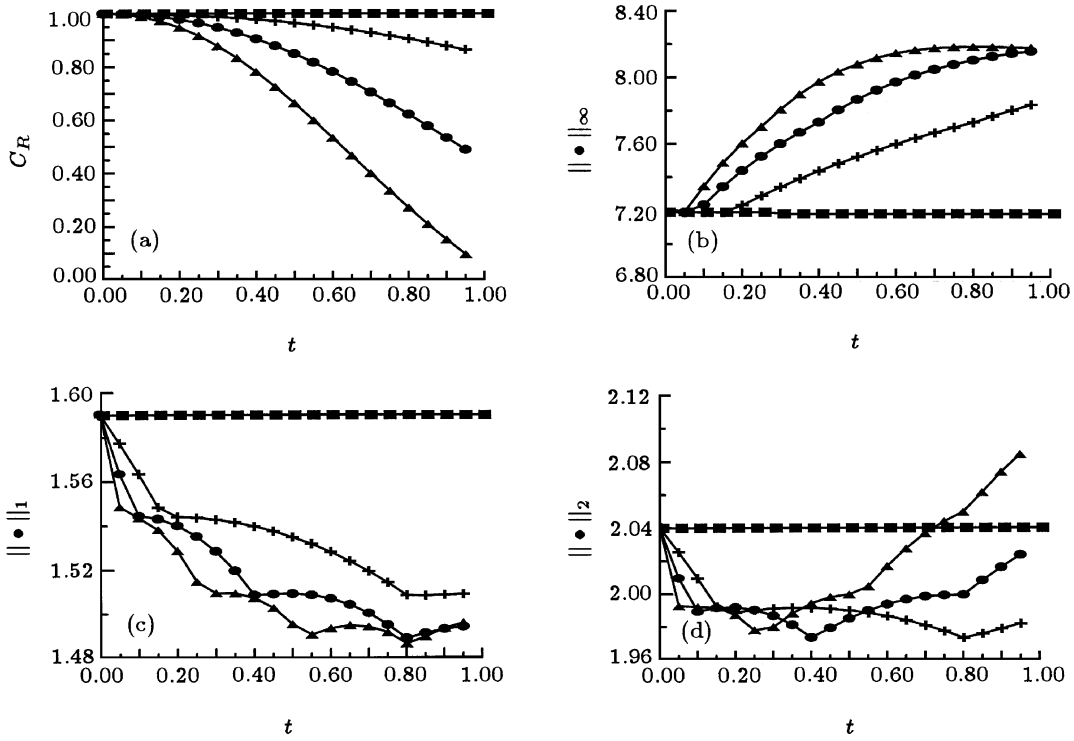


Fig.4. Temporal variations of correlation coefficients (a), and errors expressed in $\|\bullet\|_\infty$ (b), $\|\bullet\|_1$ (c), and $\|\bullet\|_2$ (d) norms in the second test, their initial field being given by Eq.(6). The time increment of the RT scheme is 0.01; those of the other schemes are 0.001. —■— RT, —+— BOTT, —●— LF2C, —▲— LF2.

The remarkable difference of the two test results is the values of the grid minimum and maximum, which are generally used to indicate the influence of the numerical dispersion and diffusion upon the total error. The grid minimum values of the second experiment are all negative, and opposite to the analytic values, thus indicating that the numerical solutions are strongly divergent, but the absolute grid minimum value obtained by the application of the RT scheme are the smallest, meaning that the RT scheme has the smallest diffusion among the four schemes.

Table 2 shows that the corresponding norms, correlation coefficients, same sign rates and greatest errors are the same in comparison with Table 1. The temporal variation tendencies of the correlation coefficient of various schemes are the same too (see Fig.4(a)). The maximum errors increase rapidly with time except that for the RT scheme, it maintains constant at 7.20 or so and among them the maximum error of the LF2 scheme increases fastest (Fig.4(b)). The temporal variation tendencies of minimal errors $\|\bullet\|_1$ and root-mean-square errors $\|\bullet\|_2$ are opposite to the first rotational flow-field test: except for the RT scheme, which maintains constant at 1.59 and 2.04, respectively, the minimal errors for other schemes reduce rapidly (Fig.4(c)), and the $\|\bullet\|_2$ errors oscillate with time (Fig.4(d)). The predicted fields of the advection equation obtained by the RT, LF2, LF2C and

BOTT schemes respectively at the end of the integration t=1 are given in Fig.5, which shows that the prediction fields with the RT and BOTT schemes are rather consistent with the ideal field (REF) at this moment, and only have some differences in details. But for the LF2C and LF2 schemes, the prediction fields have hardly any relation with the ideal field, and unfortunately many negative values have appeared.

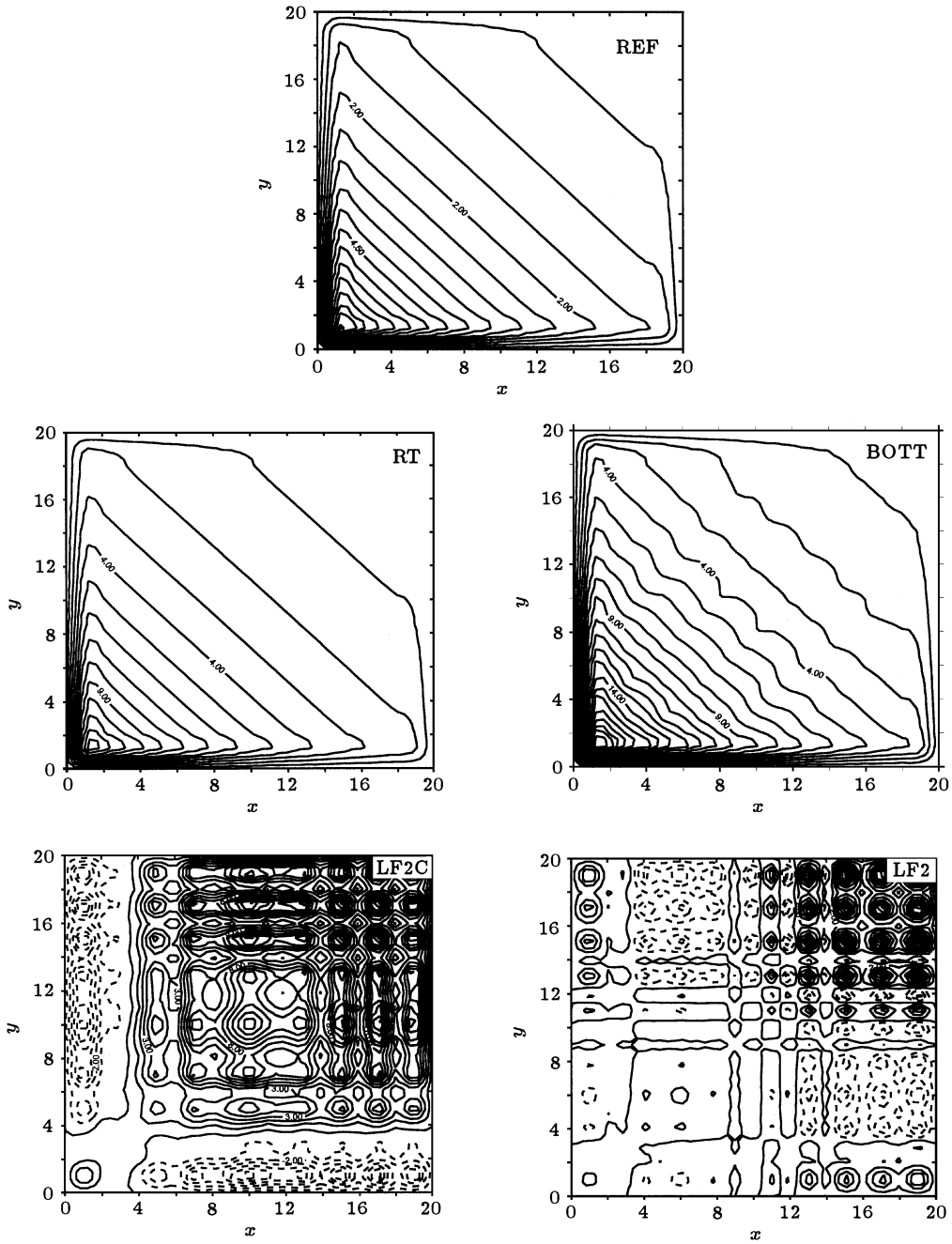


Fig.5. The analytical solution (REF) and the results of the short-term integration of Eq.(4) in the second rational flow field test integrated by using the RT, BOTT, LF2C, and LF2 schemes at the time t=1.0, representing the 1000th time step, for the RT scheme (100th time step).

The resultant numerical solutions of Eq.(4) obtained by using the four schemes at the end of integration t=500 and the analytic solution are shown in Fig.6. By comparing the analytic solution with the numerical solutions obtained by the RT and BOTT schemes, we see that they differ in details in describing the main features of the fields. The quantitative difference expressed in errors suggests that the LF2 and LF2C schemes have a significantly greater diffusion in comparison with the RT and BOTT schemes.

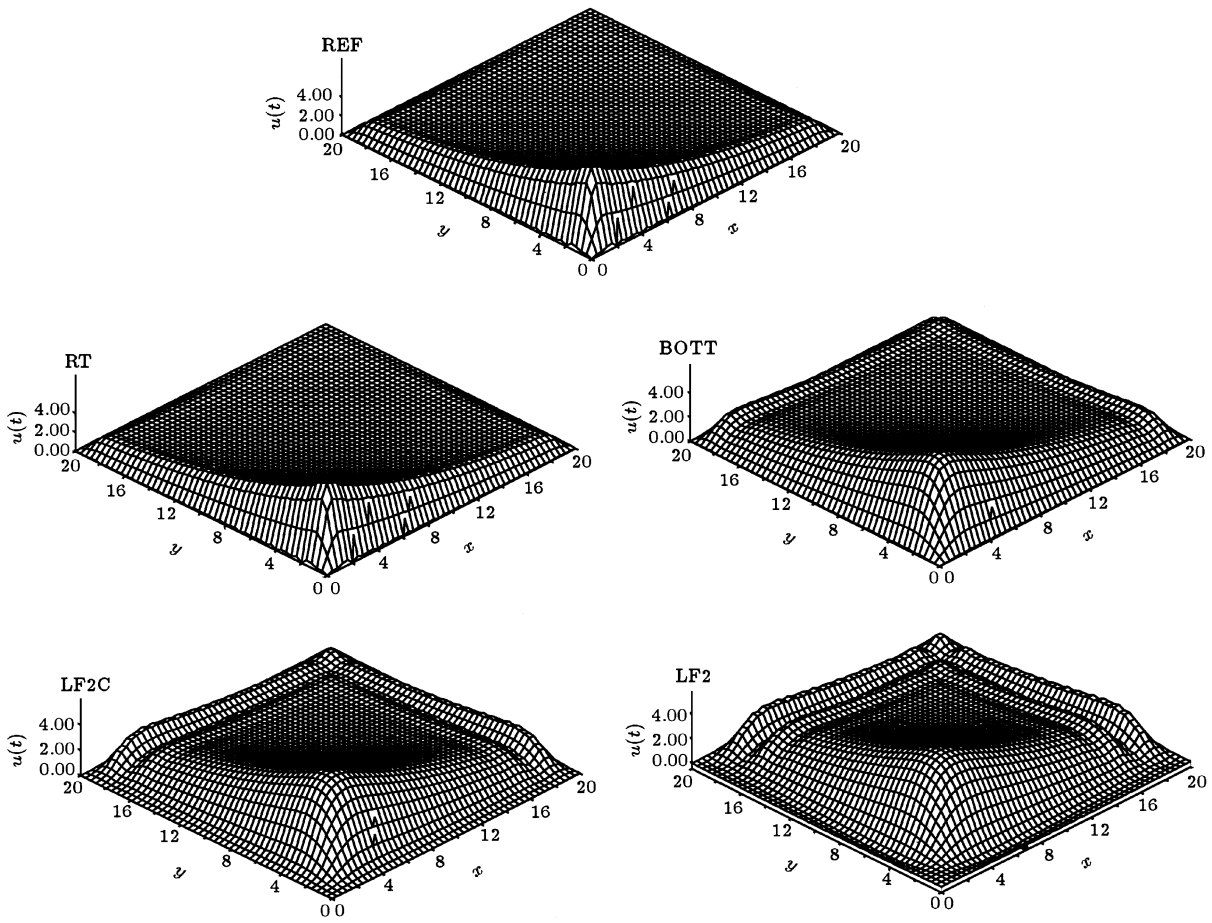


Fig.6. The analytical solution (REF) and the results of the long-term integration of Eq.(4) in the second rational flow field test integrated by using the RT, BOTT, LF2C, and LF2 schemes at the time t=500, representing the 500 000th time step, for the RT scheme (50 000th time step).

3. Conclusion

In order to evaluate the RT scheme's applicability, the LF2, LF2C and BOTT schemes used in atmospheric models were selected for comparison, and two frequently used rational flow-field tests were performed to compare the schemes' accuracy measured by the commonly used norms, the predict skills such as the correlation coefficients, the rate of same sign, and to compare their computational efficiency expressed in the time consumption. The two tests show that the worst results were obtained by the LF2 and LF2C schemes, and the BOTT scheme provided the better results due to using the highest polynomial approximation. Although the number of time steps of the RT scheme in the integration was ten times those of the other schemes, it still gave the best results in the numerical tests due to its filtering and integrating functions, and due to its utilization of the past observational data. It was found from the wavelet analysis that the periods of the predicted field obtained by the RT scheme were rather consistent with those of the initial field, indicating that the RT scheme is able to memorize the initial information. Unfortunately, the RT scheme required more computational time than the other schemes. However, in most cases, it provided more accurate results.

Acknowledgment

We wish to thank Professor Cao Hong-Xing and Professor Chou Ji-Fan for their help in this work.

References

[1] Laney B 1998 *Computational Gasdynamics* (Cambridge: Cambridge University Press)

[2] James I D 1996 *J. Mar. Syst.* **8** 237

[3] Feng S D, Zhang Q and Ren R C 2001 *Acta Phys. Sin.* **50** 1207 (in Chinese)

[4] Feng S D 2001 *Acta Phys. Sin.* **50** 1006 (in Chinese)

[5] Liu M R, Chen R H, Li H B and Keng L J 1999 *Acta Phys. Sin.* **48** 1800 (in Chinese)

[6] Cao Q J *et al* 1997 *Acta Phys. Sin.* **46** 2166 (in Chinese)

[7] Liu C J, Liu Y and Kang H W 2002 *Sci. China* (D) **32** 255 (in Chinese)

[8] Liu C J, Liu Y and Kang H W 2002 *Sci. China* (D) **45** 769

[9] Li J P, Zeng Q C and Chou J F 2000 *Sci. China* (E) **43** 449

[10] Li J P, Zeng Q C and Chou J F 2001 *Sci. China* (E) **44** 55

[11] Crowley W P 1968 *Mon. Wea. Rev.* **96** 1

[12] Piotr K S 1982 *Mon. Wea. Rev.* **110** 1968

[13] Bott A 1989 *Mon. Wea. Rev.* **117** 1006

[14] Bott A 1989 *Mon. Wea. Rev.* **117** 2633

[15] Bott A 1992 *Mon. Wea. Rev.* **120** 2592

[16] Bott A 1993 *Mon. Wea. Rev.* **121** 2637

[17] Feng G L and Dong W J 2002 *Acta Mech. Sin.* **18** 53

[18] Cao H X and Feng G L 2000 *Q J. Appl. Meteor.* **11** 249 (in Chinese)

[19] Feng G L, Cao H X, Dong W J and Chou J F 2001 *Adv. Atmos. Sci.* **18** 701

[20] Feng G L, Cao H X, Dong W J and Chou J F 2001 *Chin. Phys.* **10** 1004

[21] Jia X J, Feng G L and Cao H X 2003 *Chin. J. Atmos. Sci.* **27** 1(in Chinese)

[22] Sokol Z 1999 *J. R. Meteor. Soc.* **125** 213

[23] Smolarkiewicz P K 1989 *Mon. Wea. Rev.* **117** 2626

[24] Easter R C 1993 *Mon. Wea. Rev.* **121** 297